The Use of Topographic Wave Modes to Solve for the Barotropic Mode of a Rigid-Lid Ocean Model

C. W. HUGHES

Proudman Oceanographic Laboratory, Merseyside, United Kingdom

(Manuscript received 4 May 1995, in final form 16 November 1995)

ABSTRACT

Topographic wave modes are defined for the barotropic mode of a rigid-lid ocean, and the question is asked whether these might form an efficient basis for a description of the barotropic mode of a general ocean flow. The modes are shown to be incomplete, most particularly in their representation of barotropic potential vorticity over certain areas, so extra functions must be added to "patch up" the wave modes description. With the aid of two simple, flat bottom beta-plane models, it is shown that the form of the extra function required depends on the position of the boundaries relative to contours of planetary barotropic potential vorticity, f/H. Where all the boundaries are along contours of f/H, the extra function is simply a function of f/H and time. Where a finite stretch of boundary runs parallel to f/H contours, a further additional function can (at least sometimes) produce a complete set, but when the boundary runs parallel to f/H contours for no finite distance, there is no simple way to augment the wave modes to produce a complete set. It is shown that this incompleteness is only in the representation of barotropic potential vorticity at the boundary and causes no finite error in the streamfunction, but it seems likely that the presence of this incompleteness spoils the efficiency of the sum of wave modes as a description of a general flow. It appears that topographic wave modes are the natural modes only for systems in which the boundary (at least partially) follows contours of planetary barotropic potential vorticity, f/H. The above deficiencies vanish when enough modes are considered to resolve frictional boundary layers if the no-slip boundary condition is applied. When boundary layers are too thin to resolve, however, use of the modes to represent the difference between rotating and nonrotating responses suggests the possibility of a novel way of modeling the approach to the inviscid limit. In both these cases, however, current technology limits the practicality of the method to cases where the spatial structure of the wave modes can be calculated analytically.

1. Introduction

Many ocean models invoke the rigid-lid approximation in which the pressure at the top of the ocean is allowed to vary, but the vertical displacement of the surface that in reality produces the pressure variation is neglected. It is also common in ocean models to treat the barotropic mode (in the rigid-lid approximation, equivalent to the vertically averaged horizontal flow, with an associated vertical flow to satisfy continuity) separately from the internal flow dynamics. In this context, the natural modes of oscillation are the topographic wave modes described below. Since spectral decompositions of physical systems tend to be most efficient when the basis functions used reflect the natural variability of the system, these wave modes seem a natural choice for a set of basis functions to describe the barotropic flow in such a model. What follows is an investigation of the theoretical potential of these modes to form a complete and efficient description of the barotropic mode of an ocean flow. This problem was investigated by Greenspan (1968) for the case where lateral viscosity and a no-slip boundary condition are applied. The emphasis here is on the situation where it is impractical to resolve viscous boundary layers, and so the wave modes must represent an inviscid flow. This brings up some incompleteness problems that must be circumvented if wave modes are to be used.

2. Description of wave modes

If the linearized horizontal momentum equations are integrated vertically, making the rigid-lid approximation, the result can be written as

$$-\rho_0 \mathbf{k} \times \nabla \Psi_t + \rho_0 f \nabla \Psi = H \nabla P_b + \nabla E - \mathbf{T}, \quad (1)$$

where Ψ is the volume transport streamfunction, ρ_0 is the reference density, f is the Coriolis parameter, P is the pressure (the suffix b indicates that it is calculated at the bottom), $\mathbf{T}$ is the surface wind stress, and E is potential energy of the fluid column relative to the surface, given by

$$E = g \int_{-H}^{0} z \rho dz. \quad (2)$$

Corresponding author address: Dr. C. W. Hughes, Proudman Oceanographic Laboratory, Bidston Observatory, Birkenhead, Merseyside L43 7RA, United Kingdom.

Friction is not explicitly represented but could be included in **T** if necessary, along with nonlinear terms.

Dividing by H and taking the curl gives

$$\nabla\cdot\left(\frac{\nabla\Psi_t}{H}\right) + J\left(\Psi, \frac{f}{H}\right) = \frac{1}{\rho_0}\left[J\left(E, \frac{1}{H}\right) + \nabla\times\left(\frac{\mathbf{T}}{H}\right)\right]. \quad (3)$$

When H is constant, this reduces to

$$\nabla^2\Psi_t + \beta\Psi_x = \nabla\times\mathbf{T}. \quad (4)$$

Equations (3) and (4) have a very similar structure. A forcing on the right-hand side must be balanced by a rate of change of a circulation term and/or a volume flux across contours of (f/H or f). If the forcing is set to zero, then we have the homogeneous equations supporting free waves as follows: a volume transport across contours of (f/H or f) produces a rate of change of a quantity related to circulation. The induced circulation produces a change in the volume transport across contours, and so on. In the flat bottom case this produces Rossby waves with westward phase velocity. With topography the analogous waves are known as topographic Rossby waves, with phase propagation in a direction giving high values of f/H to the right.

Normal modes are motions periodic in time with an angular frequency ω. If such a form is imposed on the streamfunction, $\Psi = \phi e^{i\omega t}$, then (4) becomes

$$-i\omega\nabla^2\phi + \beta\phi_x = 0, \quad (5)$$

which has solutions for any ω, giving the Rossby wave dispersion relation. In an ocean basin though, ϕ must obey the appropriate boundary condition (ϕ is constant along each boundary), which turns (5) into an eigenvalue equation, soluble only for certain values of ω. Longuet-Higgins (1964) showed that the substitution $\gamma_n = \phi_n e^{ik_n x}$, $k_n = -\beta/2\omega_n$, simplifies this to

$$\nabla^2\gamma_n + k_n^2\gamma_n = 0, \quad (6)$$

the equation for normal modes of a stretched membrane held fast at the boundary. The waves, or basin modes, are thus westward-propagating sinusoids multiplied by an envelope function that is a solution of (6), assuming β can be taken as constant over the basin.

Topographic wave modes are defined, in an analogous manner, as solutions ϕ_n of

$$-i\omega_n\nabla\cdot\left(\frac{\nabla\phi_n}{H}\right) + J\left(\phi_n, \frac{f}{H}\right) = 0. \quad (7)$$

There is, in general, no substitution producing an analog of (6), but one simple type of topography on an f plane, $H = H(r)$, leads to particularly simple wave modes: $\phi_n = R_n(r)e^{in\theta}$, where n takes integer values. Term R then obeys

$$r^2R_{rr} + rR_r\left(1 - \frac{rH_r}{H}\right) - R\left(n^2 + \frac{f}{\omega_n}\frac{rH_r}{H}\right) = 0, \quad (8)$$

which takes its simplest form when H varies as a power of r. Substituting $x = \ln r$ converts this to

$$R_{xx} + R_x\left(1 - \frac{H_x}{H}\right) - R\left(n^2 + \frac{f}{\omega_n}\frac{H_x}{H}\right) = 0, \quad (9)$$

which is the equivalent equation for a topography dependent on x only and streamfunction $\Psi = R(x)\exp[i(ny - \omega_n t)]$.

The simple case, $H = H_0e^{-px}$, was solved by Buchwald and Adams (1968), and two examples of the resulting wave modes for the analogous radially symmetrical case, $H = H_0(r/r_0)^p$, are illustrated in Fig. 1. The waves are sinusoidal in the azimuthal direction and are proportional to r and $\log r$ inside and outside (respectively) the sloping region and to a sinusoid in $\log r$ multiplied by a power of r on the slope. The dispersion relation (Fig. 2) thus shows families of curves, each with different numbers of radial nodes on the sloping region, with more nodes corresponding to smaller (negative) frequency. All the waves rotate anticyclonically around the seamount, and it is possible to show (from Sturm–Liouville theory) that, with an added function of depth, they form a complete orthogonal set over the sloping region.

It is this completeness that prompted the idea of using a sum of topographic wave modes to describe the whole of the vertically integrated ocean flow. The questions that have to be answered are as follows: Do the wave modes form a complete, orthogonal set, and can the wave modes form an efficient way of describing an ocean flow?

It seems opportune to note here that, although the wave modes defined here are frictionless and linear, their use is not confined to such situations. After barotropic gravity waves and Kelvin waves, which are filtered out by the rigid-lid approximation, the fastest modes of variability in the ocean are represented by the topographic basin modes. If nonlinear and frictional terms are absorbed in **T** in (3), the use of basin modes allows a semianalytical time stepping of the barotropic mode with time steps comparable to the periods of the basin modes. It is conceivable that clever handling of the nonlinear and frictional terms could allow even longer time steps.

3. Orthogonality

Whether or not the wave modes produced in this manner are orthogonal depends on the boundary conditions assumed. For a simple, closed basin the boundary condition is ϕ_n = const, and the constant may be chosen freely (usually zero for simplicity). When there

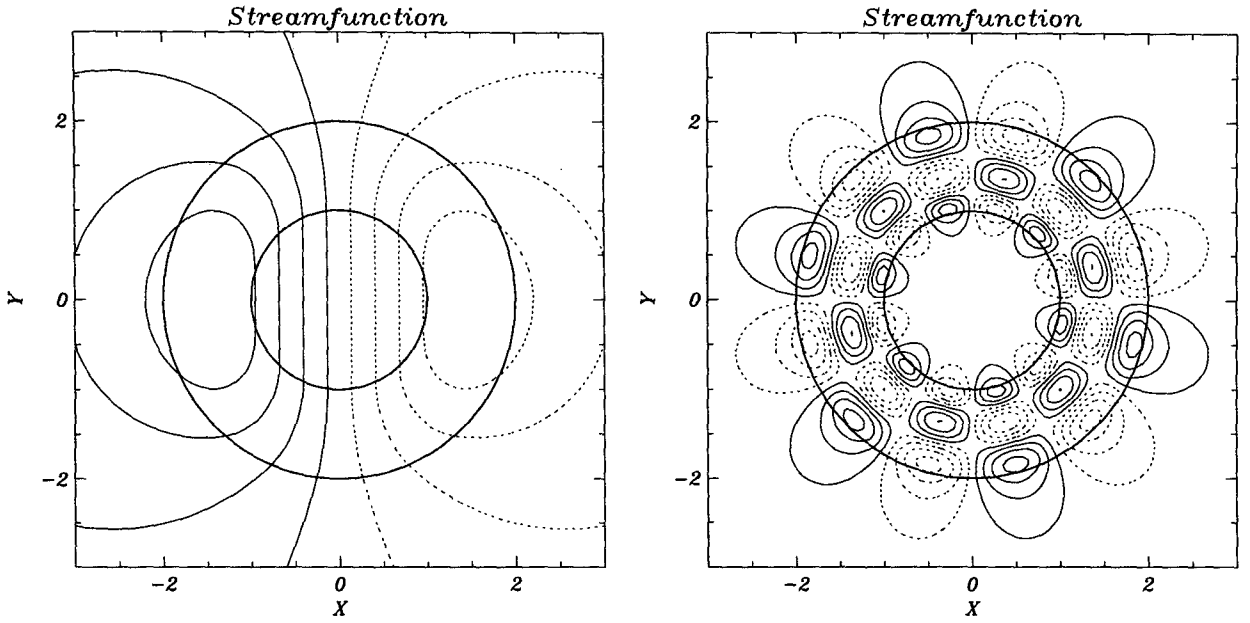

FIG. 1. Two typical topographic waves around a circular seamount. The seamount has a depth that is proportional to a power of radius, between radii 1 and 2, and is flat elsewhere with depth 3 inside radius of 1 and 5 outside radius of 2.

are islands in the domain of interest, ϕ_n can take different constant values on each boundary and the differences between values are significant, specifying the circulation around the island. In order to set the relative values, an auxiliary condition must be sought, and for this we must go back to (1). The reason for this is that the pressure field, which has been eliminated from (1) by taking the curl, must be physically realizable. Driving the flow in (3) is a force about which all we know is that it has zero curl. In a simple closed basin, zero curl implies that the force can be written as the gradient of a scalar, that is, as ∇P. When the domain includes islands, however, this is no longer true for a single-valued P. A field can have zero curl everywhere in the ocean region but may still have a circulation around each island, giving

$$\oint \nabla P \cdot d\mathbf{s} \neq 0. \tag{10}$$

Clearly, a real pressure field must be single valued. Our auxiliary boundary condition must therefore be the converse of (10):

$$\oint \nabla P \cdot d\mathbf{s} = 0. \tag{11}$$

Integrating (1) around the boundary of an island gives

$$-\rho_0 \oint \frac{\nabla \Psi_t}{H} \times d\mathbf{s} = \oint \nabla P_b \cdot d\mathbf{s} + \oint \frac{\nabla E - \mathbf{T}}{H} \cdot d\mathbf{s} \tag{12}$$

because $\nabla \Psi \cdot d\mathbf{s} = 0$ along the boundary. The bottom pressure term must integrate to zero by (11), and the second term on the right-hand side is equivalent to the forcing terms in (3), so wave modes must obey

$$\oint \frac{\nabla \phi_n}{H} \times d\mathbf{s} = 0, \quad \phi_n = \text{const}, \quad \text{on each boundary.} \tag{13}$$

The constant on the second condition is defined implicitly by the necessity to obey the first condition.

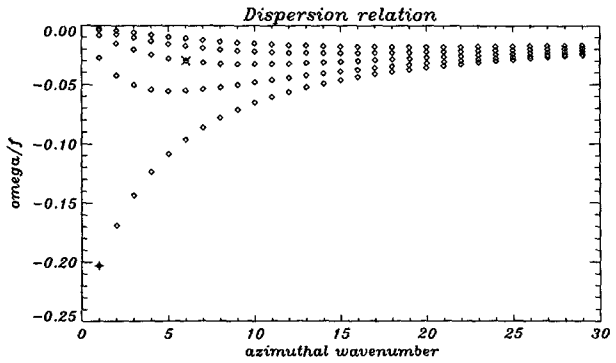

FIG. 2. Dispersion relation for shelf wave modes around the circular seamount described in Fig. 1. Wavenumber is in the azimuthal direction, with the five values at each wavenumber representing different numbers of nodes in a radial section. The largest (negative) frequency corresponds to no radial nodes, the smallest to four radial nodes. The two modes shown in Fig. 1 are marked with crosses.

Since both are linear in ϕ_n, the constant can be found by solving for two arbitrary constants and taking the linear combination of the resulting solutions that satisfies the first part of (13) (see Johnson 1989).

It is now possible to demonstrate the orthogonality of the wave modes. Taking the sum of $(7)_n \times \phi_m^* + (7)_m^* \times \phi_n$ gives

$$J\left(\phi_m^*\phi_n, \frac{f}{H}\right) + i\omega_m^*\phi_n\nabla\cdot\left(\frac{\nabla\phi_m^*}{H}\right) - i\omega_n\phi_m^*\nabla\cdot\left(\frac{\nabla\phi_n}{H}\right) = 0. \quad (14)$$

Integrating over area, the Jacobian integrates to zero since $\phi_m^*\phi_n$ is constant on each boundary, and the other two terms can be written as

$$i(\omega_n - \omega_m^*)\int \frac{\nabla\phi_n\cdot\nabla\phi_m^*}{H}\,dA + i\omega_m^*\int \nabla \times\left(\frac{\phi_n\nabla\phi_m^*}{H}\right)dA - i\omega_n\int\nabla\cdot\left(\frac{\phi_m^*\nabla\phi_n}{H}\right)dA = 0. \quad (15)$$

Use of the divergence theorem and boundary conditions (13) shows that the second and third terms integrate to zero, so

$$i(\omega_n - \omega_m^*)\int \frac{\nabla\phi_n\cdot\nabla\phi_m^*}{H}\,dA = 0. \quad (16)$$

Putting $m = n$ shows that $\omega_n = \omega_n^*$ and therefore ω_n is real. We see that it is possible to normalize the modes so that

$$\int \frac{\nabla\phi_n\cdot\nabla\phi_m^*}{H}\,dA = \delta_{nm}. \quad (17)$$

Similarly, taking $(7) \times \phi_m^*$ and integrating gives

$$\int \phi_m^* J\left(\phi_n, \frac{f}{H}\right)dA + i\omega_n\int \frac{\nabla\phi_n\cdot\nabla\phi_m^*}{H}\,dA = 0, \quad (18)$$

therefore

$$\int \phi_m^* J\left(\phi_n, \frac{f}{H}\right)dA = -i\omega_n\delta_{mn}, \quad (19)$$

giving an orthogonality relationship between the modes. This is not quite a self-adjoint system but is almost as simple since the adjoint of these functions is simply their complex conjugate.

The orthogonality relationship may also be used to put a bound on the value of ω_n. Following Johnson (1988), (19) gives us

$$i\omega_n = -\int \phi_n^* J\left(\phi_n, \frac{f}{H}\right)dA = -\int J\left(\phi_n, \frac{f\phi_n^*}{H}\right)dA + \int \frac{f}{H}J(\phi_n, \phi_n^*)dA = \int \frac{f}{H}J(\phi_n, \phi_n^*)dA = \int \frac{f}{H}\nabla\phi_n\times\nabla\phi_n^*\,dA, \quad (20)$$

but if f has amplitude everywhere less than $f_{\max}$,

$$\left|\int \frac{f}{H}\nabla\phi_n\times\nabla\phi_n^*\,dA\right| \leq f_{\max}\int \frac{\nabla\phi\cdot\nabla\phi^*}{H}\,dA, \quad (21)$$

so, using (17),

$$|i\omega_n| = |\omega_n| \leq f_{\max}. \quad (22)$$

Topographic wave modes are therefore "subinertial" in the sense defined by (22).

4. Completeness

If we assume for the moment that the set of wave modes defined above is complete, then we can calculate the response of the vertically integrated flow to a given forcing. This assumes that the forcing is not itself affected by the flow, an assumption that is not strictly true since advection of density leads to changes in E and the nonlinear and frictional terms absorbed in $\mathbf{T}$ depend on the flow. For either small amplitudes or in a steady state, the approximation should be good though. If we write the right-hand side of (3) as F and substitute for Ψ a superposition of wave modes, $\Psi = \Sigma_n \phi_n T_n(t)$, (3) becomes

$$\sum_n \frac{dT_n}{dt}\nabla\cdot\left(\frac{\nabla\phi_n}{H}\right) + J\left(\sum_n T_n\phi_n, \frac{f}{H}\right) = F. \quad (23)$$

Multiplying through by ϕ_m^* and integrating over area, using (17) and (19) reduces this to

$$\frac{dT_m}{dt} + i\omega_m T_m = -\int \phi_m^* F\,dA = -Q_m \quad \text{(say)}, \quad (24)$$

which can be integrated to give

$$T_m = T_{m0} + e^{-i\omega_m t}\int_0^t Q_m e^{i\omega_m t'}\,dt'. \quad (25)$$

Two particular cases are quite informative here. Consider a forcing that is zero before time zero and either constant (in time) or growing linearly in time after time zero. These situations correspond to models that are started with no flow and have a density field or wind stress that is either turned on at its full value at time zero or linearly increased toward its full value.

The first case gives

$$T_m = \frac{(e^{-i\omega_m t} - 1)}{i\omega_m} Q_m, \tag{26}$$

showing that a constant flow is produced, on which is superimposed a free-wave flow of equal amplitude. This is obviously quite a violent way to start a model, producing a lot of energy in the free topographic wave modes. Writing $Q_m = q_m t$ for the second case gives

$$T_m = \frac{q_m}{i\omega_m}\left(t + \frac{e^{-i\omega_m t} - 1}{i\omega_m}\right), \tag{27}$$

showing an initial oscillation of the same character as before, with a linear growth superimposed that becomes larger than the oscillatory part after a time of order $t = 1/\omega_m$. The amount of energy given to a free-wave mode is greatly diminished if the forcing is brought to its full value over a time much longer than this timescale. Notice that in both cases the forced part of the response, as opposed to the free-wave part, has the same character for every wave mode; steady for the sudden forcing and linearly growing for the increasing forcing. If the free waves are subtracted off, the remainder of the streamfunction has a constant pattern, simply growing with time in the second case.

Unfortunately, it is easy to show that, in general, the streamfunction does not behave like this. Integrating (3) over an area bounded by a closed contour of f/H, the Jacobian term disappears, giving

$$\oint \frac{\nabla\Psi_t}{H} \times d\mathbf{s} = \int F dA, \tag{28}$$

so a constant F must produce a component of Ψ that grows linearly, and a linearly growing F must produce a quadratically growing component or Ψ. The root of this problem is in the disappearance of the Jacobian term $J(\phi_n, f/H)$. In any area over which this term integrates to zero, we have

$$\int \nabla\cdot\left(\frac{\nabla\phi_n}{H}\right) dA = 0. \tag{29}$$

A sum of wave modes is therefore unable to model the distribution of the quantity $\nabla\cdot(\nabla\Psi/H)$ (barotropic potential vorticity or BPV), over such areas. These areas include regions of closed f/H contours, regions where a contour of f/H leaves a boundary and then makes its way back to the same boundary, and, indeed, regions bounded by closed boundaries that is, the whole ocean.

The obvious fix to this problem comes from the mode that has been overlooked, satisfying $\omega = 0$, $J(\phi, f/H) = 0$. This is simply the flow along contours of f/H that satisfies the unforced, steady-state equations. If we add in a function $\phi_0(f/H, t)$, we can account for all the input BPV quite easily. Over an area bounded by a contour of f/H we simply put

$$\int \nabla\cdot\left(\frac{\nabla\phi_{0t}}{H}\right) dA = \oint \frac{\nabla\phi_{0t}}{H} \times d\mathbf{s} = \int F dA, \tag{30}$$

but, since $\phi_0 = \phi_0(f/H, t)$, we have

$$\frac{\nabla\phi_{0t}}{H} \times d\mathbf{s} = \frac{1}{H}\left|\nabla\frac{f}{H}\right| \frac{\partial\phi_0}{\partial(f/H)} ds, \tag{31}$$

giving

$$\frac{\partial}{\partial t}\frac{\partial\phi_0}{\partial(f/H)} \oint \frac{|\nabla(f/H)|}{H} ds = \int F dA, \tag{32}$$

which specifies ϕ_0 if boundary values are given. The remainder of the streamfunction, $\Psi' = \Sigma_m T_m\phi_m$, now satisfies

$$\nabla\cdot\left(\frac{\nabla\Psi'_t}{H}\right) + J\left(\Psi', \frac{f}{H}\right) = F - \nabla\cdot\left(\frac{\nabla\phi_{0t}}{H}\right). \tag{33}$$

This works as long as the boundaries are all contours of constant f/H, which is almost the case away from the equator in the real ocean since the boundary is where $H \to 0$. Most models, however, have vertical walls defining the boundaries and therefore allow contours of f/H to intersect the boundary. In that case the boundary conditions disallow any finite function of f/H, but an infinitesimal function, dropping to a constant value at the boundaries, would be adequate to absorb any net BPV in a delta function of BPV generated at the boundary, without involving any finite flow. This, of course, is the situation in which a western boundary current would be generated, and for a steady state to be reached some sort of dissipation must be invoked (see Anderson and Gill 1975 for details). The continual input of BPV must be destroyed somewhere since there can be no net advection out of the region. In an ocean with density gradients and bottom topography, however, it is possible that a steady state can be reached by dynamical adjustment of bottom torques to cancel the BPV input by wind without any frictional dissipation.

A delta function of BPV at the boundary may solve the problem, but it does not seem a very elegant or efficient solution. The infinitesimal scales introduced would be expected to increase the number of wave modes necessary to resolve the flow to a given accuracy. It seems sensible to look for a more smoothly varying auxiliary function. The next simple way to absorb the net BPV is to use a function satisfying

$$\nabla\cdot\left(\frac{\nabla\Psi_{0t}}{H}\right) = F \tag{34}$$

and also satisfying the forced boundary conditions. This leaves the remainder of the solution, Ψ', to satisfy

$$\nabla\cdot\left(\frac{\nabla\Psi'_t}{H}\right) + J\left(\Psi', \frac{f}{H}\right) = -J\left(\Psi_0, \frac{f}{H}\right). \tag{35}$$

This looks like a promising candidate to be expressed as a sum of wave modes since the limitations on wave modes were due to the fact that the Jacobian term integrates to zero over a number of regions, and this time the forcing suffers from exactly the same limitations. There is a rather curious problem, though, connected with the way the boundary conditions affect the wave modes. Writing $\Psi' = \Sigma_n \phi_n T_n$ and

$$\nabla\cdot\left(\frac{\nabla\phi_n}{H}\right) = \frac{1}{i\omega_n} J\left(\phi_n, \frac{f}{H}\right) \tag{36}$$

gives

$$\sum_n \left(\frac{T_{nt}}{i\omega_n} + T_n\right) J\left(\phi_n, \frac{f}{H}\right) = -J\left(\Psi_0, \frac{f}{H}\right). \tag{37}$$

Along a boundary, ϕ_n and Ψ_0 are constant, so we may rewrite the Jacobian terms giving

$$\sum_n \left(\frac{T_{nt}}{i\omega_n} + T_n\right)\phi_{n_p}\left(\frac{f}{H}\right)_s = \Psi_{0_p}\left(\frac{f}{H}\right)_s, \tag{38}$$

where s is a coordinate measured along the boundary, and p is perpendicular to s. Wherever $(f/H)_s$ is nonzero, we have

$$\sum_n \left(\frac{T_{nt}}{i\omega_n} + T_n\right)\frac{\phi_{np}}{H} = \frac{\Psi_{0p}}{H}, \tag{39}$$

but Ψ_0 was chosen to obey the boundary condition

$$\oint \frac{\nabla\Psi_{0t}}{H} \times d\mathbf{s} = \oint \frac{\Psi_{0pt}}{H}\, ds = \int F dA \tag{40}$$

and ϕ_n to obey

$$\oint \frac{\phi_{np}}{H}\, ds = 0, \tag{41}$$

so either Ψ' cannot be represented as a sum of wave modes at the boundary or there must be some sort of singularity where $(f/H)_s = 0$. If the boundary runs parallel to f/H contours over some finite distance, the problem disappears.

Another problem is the inefficiency of this method when it is not necessary. If the forcing is steady and integrates to zero over the troublesome regions (which it must do in any steady-state ocean), a solution that could have been written as a sum of wave modes is instead written as a growing Ψ_0 plus a sum of wave modes that includes a growing portion exactly cancelling Ψ_0 and a steady portion that is the actual solution. This problem can be minimized by casting Ψ_0 onto wave modes and subtracting from Ψ_0 its wave modes representation, leaving only that part of Ψ_0 that cannot be represented as a sum of wave modes.

5. Beta-plane models

In order to examine these problems in more detail, two simple models are considered. These models take advantage of the simplicity of (6) for the Rossby wave modes of a flat-bottomed ocean.

To investigate the problem of topographic modes failing to represent the net input of BPV, a rectangular ocean is considered with boundaries running north–south and east–west. Modes for this geometry have the form

$$\phi_n = a_n \sin\left(\frac{m\pi x}{K}\right)\sin\left(\frac{n\pi y}{L}\right)e^{ik_n x} \tag{42}$$

if the basin runs from $x = 0$ to K, $y = 0$ to L. If we choose a forcing of the form $F = F_0 \sin(\pi y/L)$ so that we need not consider modes with $n \neq 1$, then the forced equation may be written

$$(\Psi_{XX} - \Lambda\Psi)_T + \Psi_X = 1, \tag{43}$$

and the mode equation becomes

$$-i\Omega_n(\phi_{nXX} - \Lambda\phi_n) + \phi_{nX} = 0, \tag{44}$$

where $X = x/K$, $T = t\beta K$, $\Omega_n = \omega_n/\beta K$, $F_0 = \beta/K$, $\Lambda = (K\pi/L)^2$ and all functions are of X only to be multiplied by $\sin(\pi y/L)$ to get the complete spatial dependence.

Equation (43) is the same as Eq. (6.4) of Anderson and Gill (1975, AG hereafter), which is a representation of a very similar problem—the spinup of an ocean by Rossby waves, but in their case with a free surface. The solution given by AG for $\Lambda = 20$ [corresponding to $\Lambda = 80$ in (43) since AG have boundaries at $X = \pm 1$ instead of $X = 0$ and $X = 1$] will be taken as a reference against which to compare sums of basin modes. This reference solution is recalculated using a Fourier decomposition of Ψ,

$$\Psi = \sum_n a_n(T)\sin(n\pi X), \tag{45}$$

which leads to a simple pair of equations for the coefficients a_n:

$$\text{for even } n,\quad a_{nT}\left[\frac{n^2\pi^2 + \Lambda}{2}\right] = \sum_{\text{odd } m} 2a_m \frac{mn}{n^2 - m^2} \text{ and} \tag{46a}$$

for odd n,

$$a_{nT}\left[\frac{n^2\pi^2 + \Lambda}{2}\right] = \sum_{\text{even } m} 2a_m \frac{mn}{n^2 - m^2} - \frac{2}{n\pi}. \tag{46b}$$

This can be efficiently timestepped by a leapfrog method since the rate of change of even coefficients depends only on the odd coefficients, and vice versa. The resulting reference solution is shown in Fig. 3.

The normalized wave modes from (44) are

$$\phi_n = \frac{1}{\sigma_n}\sin(n\pi X)e^{i\sigma_n X}, \tag{47}$$

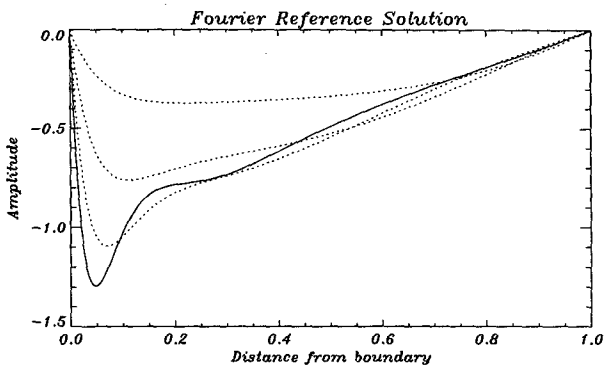

FIG. 3. Reference solution of the initial stages of spinup of a rectangular ocean. Plotted are values of Ψ from Eq. (33), with $\Lambda = 80$ as a function of eastward distance across the ocean for nondimensional times 30, 60, 90 (dotted), and 120 (solid). The different nondimensionalisation employed by AG produces a change by a factor of two in time and amplitude. The uppermost curve represents the earliest time.

where $\sigma = (\Lambda + n^2\pi^2)^{1/2}$ and $\Omega_n = -1/2\sigma_n$. From these, Ψ may be calculated in two different ways. First, assuming that the whole solution may be represented as a sum of wave modes, we put $\Psi = \Sigma_n \phi_n \Theta_n(T)$ and obtain

$$\Theta_n = \frac{n\pi}{\Lambda\sigma_n}\left(\frac{1 - e^{-i\Omega_n T}}{i\Omega_n}\right)(1 \pm e^{-i\sigma_n}), \qquad (48)$$

where the positive sign is taken when n is odd and the negative sign when n is even. The second method is to absorb the BPV into a function Ψ_0 satisfying

$$(\Psi_{0XX} - \Lambda\Psi_0)_T = 1 \qquad (49)$$

and to write the remainder of the solution as $\Psi' = \Sigma_n \phi_n \Theta_n(T)$, which gives

$$\Psi_0 = T\left\{\frac{\cosh[(X - 0.5)\Lambda^{1/2}]}{\Lambda \cosh(0.5\Lambda^{1/2})} - \frac{1}{\Lambda}\right\}, \qquad (50a)$$

$$\Theta_n = \frac{n\pi}{\Lambda\sigma_n}\left(\frac{1 - e^{-i\Omega_n T}}{i\Omega_n} - T\right)(1 \pm e^{-i\sigma_n}). \qquad (50b)$$

The ability of these two approximations to represent the true solution is tested by calculating them for $T = 120$ and subtracting them from the Fourier solution to see how the residuals behave. Two such cases are shown in Fig. 4: the first for a sum of 30 wave modes, and the second for a sum of 60 wave modes. Both cases show the same general features. The residual in all cases oscillates with the wavenumber of the first uncalculated mode. In addition, the residual for the sum of wave modes only has in each case a constant offset from zero, which is inversely proportional to the number of modes. This constant offset represents the net BPV, concentrated in a region whose extension away from the boundary is limited to the length scale of the first uncalculated mode. In the limit of an infinite number of wave modes, this may be interpreted as the infinitesimal function of f/H mentioned earlier. In addition to avoiding this constant offset, the solution in which the net BPV input is handled separately has the advantage that the oscillatory part of the residual is smaller in amplitude (and increasingly so as the number of modes is increased) than the oscillatory part of the residual in the pure wave mode case. In short, when the wave modes alone are used to represent the solution, they suffer from something akin to a Gibbs phenomenon that increases the number of wave modes needed for a given accuracy. This problem is avoided if the net BPV is treated separately, and the wave modes are used only to represent the difference be-

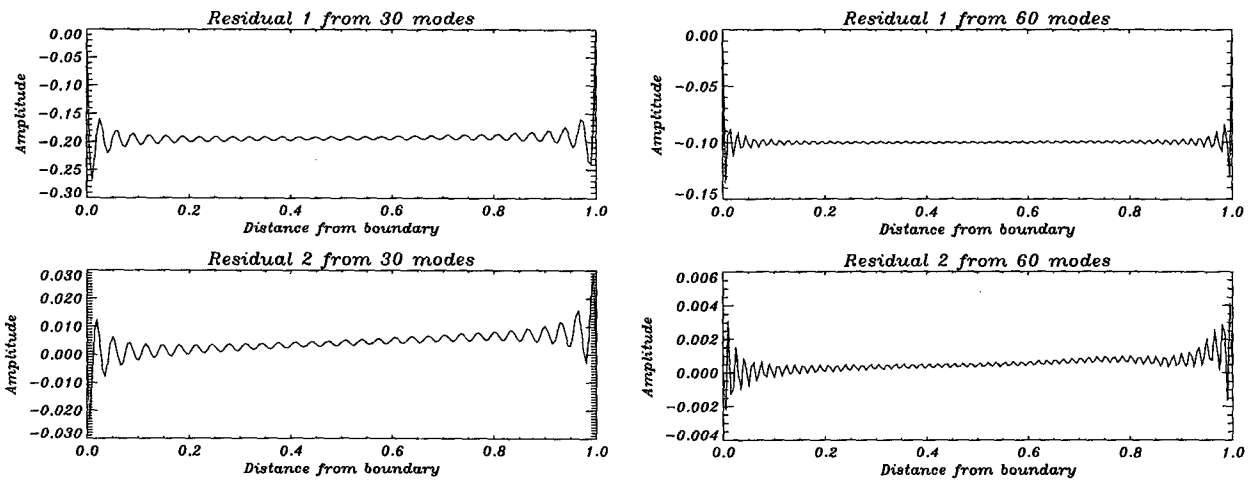

FIG. 4. Differences between streamfunctions calculated as a sum of wave modes and an accurate solution found by time-stepping Fourier modes. Residual 1 is calculated purely as a sum of wave modes and residual 2 is a solution that considers the net input of BPV separately. (a) Using 30 wave modes. (b) Using 60 wave modes. Note the different vertical scales.

tween the solution for a nonrotating ocean and that for a rotating ocean.

Another way of looking at this is that the singularities introduced by using a description in terms of a sum of wave modes plus a function of f/H produce a small-scale input to the forcing of the wave modes and thus increase the number of modes needed to resolve the solution. The function of f/H was not included explicitly in this calculation, but it only forces the topographic modes with a delta function at the boundary, and since the modes all go to zero at the boundary, this forcing is not cast onto the modes at all. Assuming the solution can be expressed purely as a sum of wave modes is therefore equivalent to adopting an infinitesimal function of f/H to absorb the net BPV.

We cannot use this model to look at the boundary condition problem since the rectangular ocean has northern and southern boundaries that run parallel to contours of f/H. We must therefore move to a slightly more complex basin shape: a square with boundaries at 45° to the north–south direction. If the x and y axes are chosen as in Fig. 5 and the basin has sides of length K, then, nondimensionalizing so that $X = x/K$, $Y = y/K$, $T = t\beta K/\sqrt{2}$, and choosing a simple, doubly sinusoidal forcing produces the equation

$$(\Psi_{XX} + \Psi_{YY})_T + \Psi_X + \Psi_Y = \sin(\pi X)\sin(\pi Y), \quad (51)$$

and for the wave modes,

$$-i\Omega(\phi_{XX} + \phi_{YY}) + \phi_X + \phi_Y = 0. \quad (52)$$

The normalized wave modes for this equation are

$$\phi_{mn} = \frac{1}{\sigma_{mn}} \sin(m\pi X)\sin(n\pi Y)e^{i\sigma(X+Y)}, \quad (53)$$

with $\sigma_{mn} = \pi[(m^2 + n^2)/2]^{1/2}$, $\Omega_{mn} = -1/2\sigma_{mn}$.

Writing $\Psi_0 = \Psi_1 T$, we have

$$\nabla^2\Psi_1 = \sin(\pi X)\sin(\pi Y), \quad (54)$$

which may be solved immediately giving

$$\Psi_1 = \frac{-1}{2\pi^2} \sin(\pi X)\sin(\pi Y). \quad (55)$$

This gives us

$$\nabla^2\Psi'_T + \Psi'_X + \Psi'_Y = -\frac{T}{2}(\Psi_{1X} + \Psi_{1Y})$$

$$= \frac{T}{4\pi}[\cos(\pi X)\sin(\pi Y) + \sin(\pi X)\cos(\pi Y)]. \quad (56)$$

The essential problem is in representing the right-hand side as a sum of Jacobians of wave modes, so, for the purpose of investigation, the left-hand side can be replaced by $\nabla^2\Psi'$, which has a simpler form but will suffer from the same difficulty in being represented as a sum of wave modes (this in fact produces the component of Ψ that grows initially as T^2). Writing the cosine terms as a Fourier series of sines, the ∇^2 operator may then be inverted, again giving

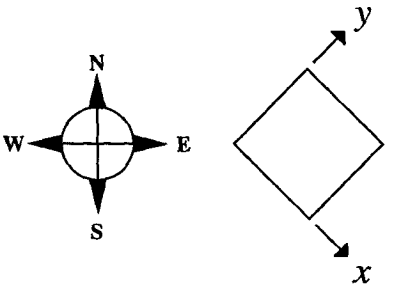

FIG. 5. Diagram to show the orientation of axes used in the second beta-plane model.

$$\Psi' = \frac{-T}{\pi^4} \sum_{\text{even } m} \frac{m}{m^4 - 1} \times [\sin(\pi Y)\sin(m\pi X) + \sin(\pi X)\sin(m\pi Y)], \quad (57)$$

which, happily, turns out to be a sum over only one index.

Writing Ψ' as a sum of wave modes produces, after a fair amount of algebra,

$$\Psi' = \frac{T}{2\pi^4} \sum_{m,n} \text{Re}\left[\frac{i\alpha\alpha_2}{\sigma_{mn}} \frac{(1 \pm e^{-i\sigma_{mn}})(1 \pm e^{-i\sigma_{mn}})}{(\alpha^2 - \beta^2)(\alpha_2^2 - \beta_2^2)} \times \sin(m\pi X)\sin(n\pi Y)e^{i\sigma_{mn}(X+Y)}\right], \quad (58)$$

where $\alpha = 2m$, $\alpha_2 = 2n$, $\beta = 1 + (m^2 - n^2)/2$, $\beta_2 = 1 + (n^2 - m^2)/2$, and a plus sign is taken for each of m and n that is even.

Figure 6 shows Ψ' calculated from (57) at $T = 1$ and the difference between Ψ' from (57) and Ψ' from (58). A problem near the east and west corners is apparent, although the size of the residual is actually quite small. The maximum residual decreases as the number of modes used increases (from $\pm 1.52 \times 10^{-5}$ for 10×10 modes to $\pm 3.80 \times 10^{-6}$ for 20×20 modes), so the representation of streamfunction seems to be convergent, and the residual looks like a two-dimensional version of Fig. 4, with a small oscillation at the wavenumber of the first missed modes amplified toward the eastern and western corners.

It might be objected that the representation of the cosine terms in (56) as a Fourier series of sines is not valid since such a series must produce a Ψ' such that $\nabla^2\Psi' = 0$ at the boundary. It is certainly true that the Fourier series cannot converge to the correct $\nabla^2\Psi'$ at the boundary, but it is clear from the properties of Fourier series that it will converge to the correct value everywhere else, and, when integrated twice, the misfit at

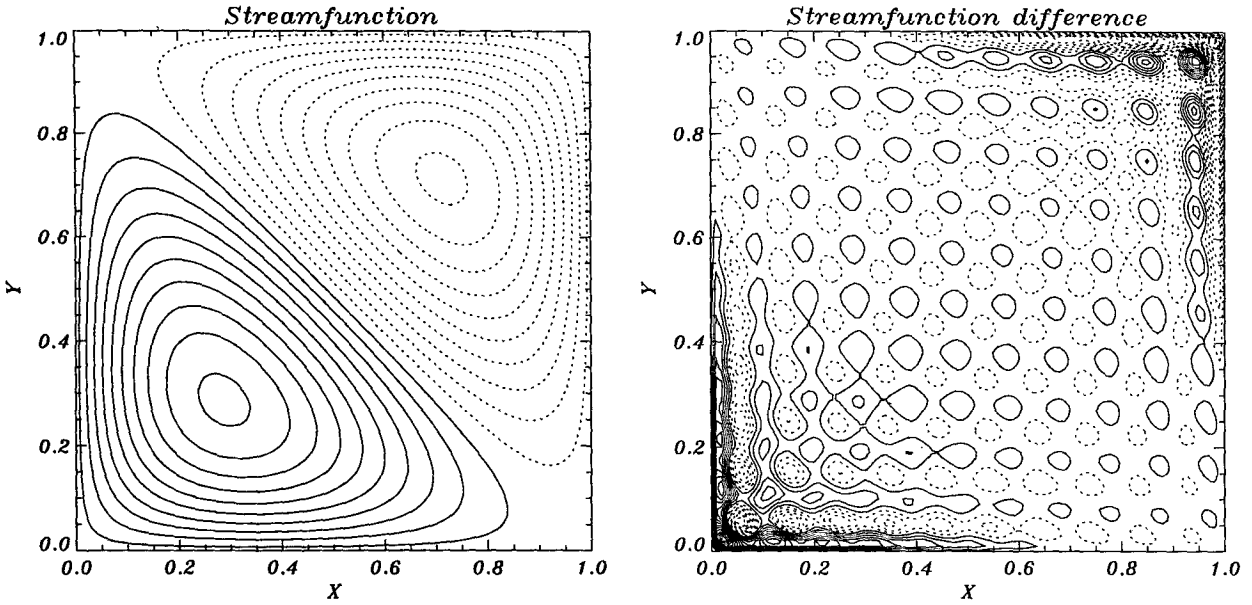

FIG. 6. (a) The streamfunction Ψ' calculated from Eq. (57) as a solution of (part of) Eq. (56) (the version calculated as a sum of wave modes is not visibly different). Extreme values are $\pm 1.94 \times 10^{-3}$ with a contour interval of 2×10^{-4}. (b) The difference between Ψ' in (a) and the version calculated as a sum of wave modes. Extreme values are $\pm 1.52 \times 10^{-5}$ with a contour interval of 1×10^{-6}. Negative contours are dotted.

the boundary can have no finite effect on the value of the streamfunction. The streamfunction itself has no such problem since the Fourier sinusoids obey the true boundary condition of the problem, $\Psi' = 0$ at the boundaries.

The small length scale of the residual means that the relative size of the residual will be larger for BPV than for streamfunction, raising the possibility that the sum might not be convergent in BPV. This is what we suspect happens at the boundary in order to resolve the boundary condition constraint. The value of $\nabla^2\Psi'$ from (58) and the analytical form

$$\nabla^2\Psi_2 = \frac{-1}{4\pi}[\cos(\pi X)\sin(\pi Y) + \sin(\pi X)\cos(\pi Y)] = \frac{-1}{4\pi}\sin[\pi(X+Y)] \tag{59}$$

has been calculated along sections at the boundary ($X = 0$) and at $X = 0.5$ (Fig. 7). This figure shows sums of 5×5, 10×10, 15×15, and 20×20 wave modes, and the dashed curve shows the true analytical value. It is clear from Fig. 7a that $\nabla^2\Psi'$ at the boundary converges to a value that is wrong by a finite amount of the same order as the true value, but Fig. 7b shows that this is not the case away from the boundary, with $\nabla^2\Psi'$ converging to the true value everywhere except $Y = 0$, $Y = 1$.

With this result as a guide, we can see how to generalize to a basin of any shape with topography. We have

$$\nabla\cdot\left(\frac{\nabla\Psi_t}{H}\right) + J\left(\Psi, \frac{f}{H}\right) = F, \tag{60}$$

$$\oint \frac{\nabla\Psi_t}{H} \times d\mathbf{s} = \int F dA. \tag{61}$$

We now write $\Psi = \Psi_0 + \Psi'$, where

$$\nabla\cdot\left(\frac{\nabla\Psi_{0t}}{H}\right) = F + \delta F, \tag{62}$$

$$\oint \frac{\nabla\Psi_t}{H} \times d\mathbf{s} = \int F dA, \tag{63}$$

$$\nabla\cdot\left(\frac{\nabla\Psi'}{H}\right) + J\left(\Psi', \frac{f}{H}\right) = -J\left(\Psi_0, \frac{f}{H}\right) - \delta F. \tag{64}$$

If δF is chosen to have a finite value at the boundary, so as to eliminate the problem of representing Ψ' as a sum of wave modes but to be zero elsewhere so that $\int \delta F dA = 0$ over any area, then δF produces no change in the coefficients of the wave modes since it must be integrated to produce them, and similarly there is no change in Ψ_0. The only difference is a finite change in $\nabla\cdot(\nabla\Psi_0/H)$ right at the boundary of amplitude $\int_0^t \delta F dt'$, which can only alter the flow in the inviscid case, as $t \to \infty$. It appears that the Gibbs phenomenon has returned and that the lack of a finite length of boundary parallel to contours of f/H again requires that a function of BPV be added along the boundary in order to make the sum of wave modes plus Φ_0 complete in

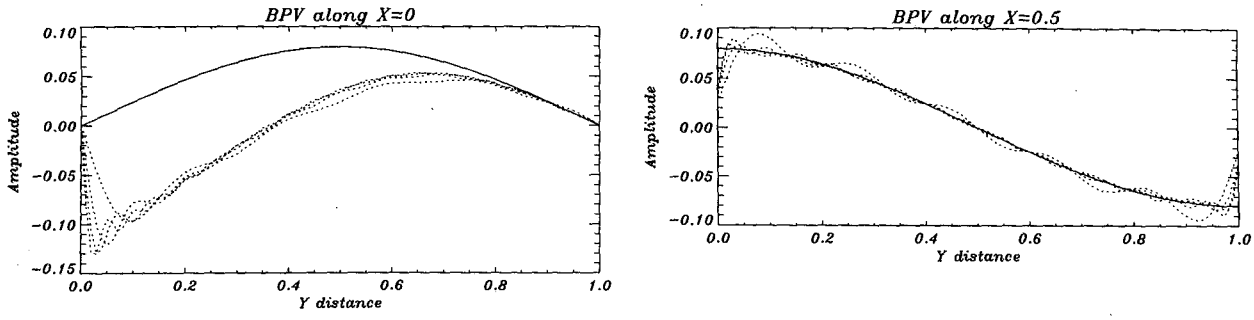

FIG. 7. $\nabla^2\Psi'$ calculated at (a) $X = 0$, that is, the northwestern boundary, and (b) $X = 0.5$. The y axis is distance in the Y direction (northeast). Each figure shows five curves: solutions calculated as a sum of 5×5, 10×10, 15×15, and 20×20 wave modes shown dotted, and a solid curve showing the analytical solution.

its representation of BPV. In this case, though, the function is finite.

6. Friction

Up to this point the talk has been of using the inviscid normal modes to solve the inviscid problem. It is well known that this problem involves an ever-narrowing western boundary layer and never reaches a steady state. The resolution of this problem is thoroughly discussed by Greenspan (1968) and involves an inertial boundary layer with a frictional boundary layer embedded within it, although it is not clear how important the frictional boundary layer is when realistic bottom topography is considered.

In terms of wave modes, if enough modes are considered to resolve the boundary layers, then the difficulties discussed above disappear. The reason for this is that a narrow boundary layer can now form in which friction produces BPV that can cancel the net BPV input from elsewhere. For example, when lateral friction is included, the no-slip condition ensures that BPV integrated over the whole ocean is zero, so the inability of wave modes to resolve this component of BPV is irrelevant. Similarly, the no-slip condition solves the curious boundary problem since it results in $\Psi_{0p} = 0$ in (38). When enough modes can be considered to resolve viscous boundary layers, they seem to offer a good natural basis for an ocean model. The obvious problem is the memory requirement, which with current technology makes the use of topographic modes for high resolution impractical except for basin shapes for which the modes can be calculated analytically. In the latter case, however, they do offer the possibility of long time steps, which may be useful in the study of thermohaline circulations.

Perhaps more interesting, though, is the behavior of a modal representation of the flow in the limit of small viscosity. If internal viscous boundary layers are assumed to be unimportant, the viscous effects can all be contained in the function Ψ_0 and are limited to a vanishingly small region near the boundary. Nonetheless, this boundary layer is sufficient to remove the constraints of net BPV representation, as well as the boundary problem. With stratification and bottom topography, it may be possible for a truncated model of this kind to reach a statistically steady state. Such a model would be a useful addition to our current armory in trying to understand the effects of viscosity in the ocean.

7. Conclusions

The incompleteness of topographic wave modes has been shown to be most obvious in their inability to represent net BPV integrated over certain regions of the ocean, such as those bounded by closed contours of f/H. When the boundaries of the region in question are parallel to contours of f/H, this deficiency is easily remedied by adding a function of f/H and time, which is effectively a set of additional modes with zero frequency. When contours of f/H run into the boundary, however, things are more complicated. This situation has been explored by means of two simple, beta-plane models. The first of these models has northern and southern boundaries parallel to contours of f/H but eastern and western boundaries intersecting the contours. In this case, the approximate solution calculated as a sum of wave modes converges to the true solution except that its representation of BPV at the boundary remains wrong by a finite amount. An alternative solution, in which the net BPV is absorbed by an extra function, Ψ_0, and the wave modes are used to represent the difference between Ψ_0 and the true solution, is shown to converge more rapidly and without the failure to represent BPV at the boundary.

Unfortunately, it was shown that a finite stretch of boundary parallel to f/H contours is a special case in which Ψ_0 can resolve a second possible difficulty in representation of the BPV as a sum of wave modes. To investigate a more generic case, a second beta-plane model was used in which the f/H contours are not par-

allel to any finite stretch of boundary. With this model it was shown that the addition of Ψ_0 can no longer resolve this second difficulty, and a sum of Ψ_0 plus wave modes again fails to represent BPV at the boundary. The small scales thus introduced raise a serious question about whether wave modes can form an efficient description of the flow in such a case.

The above problems vanish when enough modes are considered to resolve a viscous boundary layer, making wave modes a good basis for an ocean model when they can be calculated analytically. On the other hand, the inclusion of a small viscosity can produce boundary layers that are not resolved by a truncated set of modes. In this case, a modal representation of the difference between rotating and nonrotating responses to sources and sinks of BPV (when frictional, nonlinear, and bottom torque terms are included in the sources and sinks) behaves well at finite truncation and may offer an interesting method of approaching the inviscid limit in an ocean model, although again being currently limited to cases where the modes can be calculated analytically.

Acknowledgments. This work was done at the Robert Hooke Institute, Oxford, as part of a Ph.D. for the Department of Atmospheric, Oceanic, and Planetary Physics, Oxford University, and was supported by a Natural Environment Research Council Grant as part of the FRAM Community Research Project. I would like to thank Peter Killworth for much help and encouragement and John Huthnance and Ted Johnson for useful suggestions. An anonymous reviewer also made an important contribution.

REFERENCES

Anderson, D. L. T., and Gill, A. E., 1975: Spin-up of a stratified ocean, with applications to upwelling. *Deep-Sea Res.*, **22,** 583–596.

Buchwald, V. T., and Adams, J. K., 1968: The propagation of continental shelf waves. *Proc. Roy. Soc. London, Ser. A,* **305,** 235–250.

Greenspan, H. P., 1968: *The Theory of Rotating Fluids.* Cambridge University Press, 327 pp.

Johnson, E. R., 1988: Topographic waves in open domains. Part 1. Boundary conditions and frequency estimates. *J. Fluid Mech.*, **200,** 69–76.

——, 1989: Scattering of shelf waves by islands. *J. Phys. Oceanogr.*, **19,** 1311–1316.

Longuet-Higgins, M. S., 1964: Planetary waves on a rotating sphere. *Proc. Roy. Soc. London, Ser. A,* **279,** 446–473.